CHAPTER III

CHITOSAN CORE-CORONA NANOSPHERES: A CONVENIENT MATERIAL TO TAILOR pH AND SOLVENT RESPONSIVE MAGNETIC NANOPARTICLES

3.1 Abstract

Chitosan nanospheres (CSNS) with a core-corona structure containing hydrophobic phthaloyl group and a hydrophilic poly(ethylene glycol) group perform as the backbone to allow interaction with magnetite nanoparticles (MAG). Having hydrophilic corona favors the coverage of MAG on the CSNS surface to form CSNS-MAG. In contrast, having hydrophobic core allows the incorporation with MAG if the MAG is in the form of oleic acid coated MAG (O-MAG) to form CSNS-O-MAG. In the case of CSNS-MAG, the dispersion of MAG on the CSNS surface is easily tunable and at that time the MAG content on CSNS is also variable under pH condition, so-called pH responsive CSNS-MAG. The CSNS-MAG is well-dispersed and stabilized in colloidal state in aqueous and polar solvent and this brings to the size adjustable CSNS-MAG, so-called solvent responsive CSNS-MAG. The present work shows how core-corona chitosan is a convenient material to hybridize with MAG not only because it allows the interaction either with the hydrophilic MAG or with the hydrophobic MAG (i.e. O-MAG), but also because it provides the selective conditions to control the MAG content as well as the stability of the nanospheres in the media.

Keywords: Magnetic Nanoparticles; Chitosan Nanospheres; Responsive Material

3.2 Introduction

Recently, iron oxide or magnetic nanoparticles (MAG) have attracted much attention due to their magnetic responsive performance and biocompatibility, allowing them to be used for advanced applications. For example, they have been used as a drug delivery system (DDS), as a magnetic resonance imaging (MRI) agent, as a cancer treatment hyperthermia, and for nucleic acid adsorption [1-4]. However, the fact that nanoparticles tend to aggregate and sediment has resulted in MAG having a short life time. In the past, stabilization of MAG in media by means of coating the particles with surfactants or organic molecules [5-8], or as well as by encapsulating them in polymeric chains [9-11], by modifying the surface with silane coupling agents [12-14], and by conjugating the particles with functional molecules [15-18]. Considering the applications related to bio-systems, encapsulating and/or conjugating with biopolymers to obtain biocompatibility while maintaining its well-dispersibility is important. In the past, polysaccharides such as -alginate, hyaluronic acid, chitosan, etc. were reported as potential biopolymers. Attempts to hybridize MAG with those polysaccharides via the secondary forces or the covalent bonds were carried out as seen in the cases of MAG with alginate [19, 20], MAG with hyaluronic acid [21], and MAG with chitosan [5, 6, 11, 18].

Chitosan is a natural abundant amino-polysaccharide containing reactive (amino and hydroxyl) functional groups. The unique amino-polysaccharide structure results in chitosan becoming cationic, biodegradable, biocompatible, non-toxic in solution at biological pHs, and chemically modifiable. Based on chitosan's amino group (pKa at ~ 5.8), several studies have reported success in developing chitosan for drug delivery with various sizes and morphology by varying the pH [22-25]. In many cases, the morphology of chitosan materials have been altered from flakes or powder to form gels, films, or even nano-sized whiskers resulting in functional materials [26-32]. Modifications of chitosan to organo-soluble species such as *N*-pthalimido chitosan [33], iodochitosan [34], and water-soluble species such as carboxymethyl chitosan [35], phosphorylated chitosan [36, 37], and *O*-succinyl chitosan [38], are known as the derivatives for materials on purposes. Recently, our group succeeded in modifying chitosan with a good balance of hydrophilic and hydrophobic groups to

obtain core-corona structural chitosan nanospheres (CSNS) [31, 32]. The size and the stability of these CSNSs were proven to be responsive with solvent polarity and pH. For example, by varying the pH from 4 to pH 12, the CSNS changed size from 300-400 nm to 20 nm, respectively [39, 40].

On the viewpoint of MAG hybridized with chitosan, the hybridization of MAG and chitosan can be achieved either via secondary interaction such as ionic interaction, hydrophobic-hydrophobic van der Waals forces, hydrogen bond or the covalent bond. Although the covalent bond system allows us precisely controlling the structure, the multi-step preparations, the time-consumption purification, and the quality control, and the yields fluctuation always obstruct the practical preparations. Hybridizing MAG with chitosan by using chitosan-salt in acidic solutions has been shown to be a simple preparation [41-43]. However, because those systems require acidic conditions, the effect of acids on MAG formation, the stability of MAG hybridized on chitosan, the disturbance of salts or acids in the systems are the complications when considering the application of the materials. It should be noted that most studies focused only on the use of chitosan as a biopolymer to uniformly distribute MAG while few considered the use of chitosan to initiate MAG with specific property of chitosan, especially pH responsiveness. The above-mentioned unique properties of our CSNS allows for the possibility to develop MAG with responsive property by applying CSNS as a biopolymer backbone for hybridization with MAG. The use of CSNS will not only satisfy the simple non-covalent bond hybridization but also may achieve the pH and solvent responsive material. Therefore, the present work aims to develop MAG hybridized with CSNS and clarify (i) the structure and morphologies of CSNS-MAG (ii) the factors and conditions to govern CSNS-MAG stability, and (iii) the specific properties in terms of pH and solvent responsiveness. The formation of CSNS-MAG will also be a model of external stimuli responsive inorganic-polymer nanoparticles under the concept of the stabilization of inorganic nanoparticles onto hydrophobic core- hydrophilic corona structured polymer.

3.3 Experimental

3.3.1 Materials

Chitosan (85% DD, M_w of 7.0 x 10^5) was obtained from Seafresh Chitosan (Lab) Co., Ltd., Thailand. 1-Hydroxybenzotriazole monohydrate (HOBt·H_2O) and 1-ethyl-3-(3-dimethylaminopropyl-carbodiimide) hydrochloride (EDC·HCl) were purchased from Tokyo Chemical Industry Co., Ltd., Japan. Phthalic anhydride, polyethylene glycol monomethyl ether (mPEG, M_n = 5 000), and succinic anhydride were purchased from Fluka Chemika, Switzerland. Iron (II) sulfate hexahydrate (99%) and iron (III) chloride heptahydrate (98%) were purchased from BDH chemicals. Sodium hydroxide was purchased from Carlo, Italy. Oleic acid was purchased from Sigma-Aldrich, USA. *N*,*N*′-dimethylformamide (DMF), isopropanol, tetrahydrofuran (THF), toluene, and ethanol were purchased from LabScan, Ireland. All chemicals were used without further purification.

3.3.2 Magnetic Nanoparticles (MAG) and Oleic Acid-coated Magnetic Nanoparticles (O-MAG)

Magnetic nanoparticles (MAG) were prepared based on a previous report from Laurent et al. with some modification [44]. Briefly, Fe^{2+} and Fe^{3+} ions (1:2 molar ratio) were co-precipitated in NaOH (2 mol L^{-1}). The MAG obtained were washed several times by distilled, de-ionized, and de-oxygenated water until obtaining a neutral pH. Finally, the MAG were stored at the concentration of 0.04 mg mL^{-1} at 4 °C.

For O-MAG, $FeCl_2$•$4H_2O$ (9.94 g, 0.05 mol) and $FeCl_3$•$6H_2O$ (27.03 g, 0.10 mol) were mixed in distilled, de-ionized, and de-oxygenated water (200 mL) under a N_2-atmosphere for 30 min. Oleic acid (20 mL) was gradually introduced dropwise and the mixture was heated at 50 °C for 15 min. Ammonia solution was added by injecting from a septum until the pH was in the range of 10–11. The mixture was heated at 80 °C for 30 min. The black precipitates were washed thoroughly in dialysis tube (MW cut-off = 12,000 Da) against de-ionized water until

the ammonia smell disappeared. Finally, the water was removed from the oleic acid-coated MAG (O-MAG) by freeze-drying.

FTIR (KBr, ν cm^{-1}): 2922, and 2851 cm^{-1} (C-H stretching), 588 cm^{-1} (Fe-O).

3.3.3 Preparation of Chitosan Nanospheres (CSNS)

Chitosan nanospheres (CSNS) were prepared as reported by Yoksan et al. [31, 32]. Briefly, chitosan (%DD = 85, 3.0 g) was reacted with phthalic anhydride (13.28 g, 5 mol equivalent to pyranose rings) in DMF (30 mL) at 100 °C under vacuum until the solution became clear. The solute was reprecipitated in cold water. The precipitates were collected and dried in a vacuum to obtain phthaloylchitosan (PhCS).

FTIR (KBr, cm^{-1}): 3469 (OH), 2640 (free carbonyl), 1777 and 1712 (C=O anhydride), 1261-1287 (C-O-C in ester), and 721 (aromatic ring).

NMR (500 MHz, DMSO-d6) δ = 3.2-5.0 (H2-H6 of GluN unit in chitosan), 2.1 (OCH_3), 5.5 (H1 of GluN of chitosan), and 7.4-8.3 (C_6H_5).

Methoxy-terminated polyethylene glycol (mPEG, M_n = 5 000 Da, 3 g, 0.0006 mol) was reacted with succinic anhydride (0.15 g, 1 mol equivalent to mPEG) with a catalytic amount of pyridine at 60 °C overnight. The solution obtained was concentrated and reprecipitated in diethyl ether to obtain mPEG-COOH.

FTIR (ZnSe, cm^{-1}): 3494 (OH), 2871 (C-H stretching), 1736 (C=O), and 1113 (C-O-C).

PhCS (0.3 g, 0.0012 mol) was stirred with mPEG (2.38 g, 0.4 mol equivalent to PhCS) in DMF (20 mL) before adding HOBt (0.19 g, 3 mol equivalent to mPEG) and stirring at room temperature until the solution became clear. 1-Ethyl-3-(3-dimethylaminopropyl) carbodiimide hydrochloride (EDC·HCl, 0.27 g, 3 mol equivalent to mPEG) was added and stirred overnight. The mixture was dialyzed against distilled water using a cellulose membrane (12 400 molecular weight cut off) to obtain CSNS. The product was collected by centrifugation, followed by washing with distilled water and ethanol, before drying in a vacuum. The synthesis steps of CSNS are shown in Scheme 1.

FTIR (KBr, cm^{-1}): 3469 (OH), 2 990 (C-H stretching), 1777 and 1712 (C=O anhydride), and 721 (aromatic ring).

NMR (500 MHz, D_2O) δ = 3.2-5.0 (H2-H6 of GluN unit in chitosan), 2.1 (OCH_3), 5.5 (H1 of GluN of chitosan), and 7.4-8.3 (C_6H_5).

Scheme 3.1 Synthesis of CSNS.

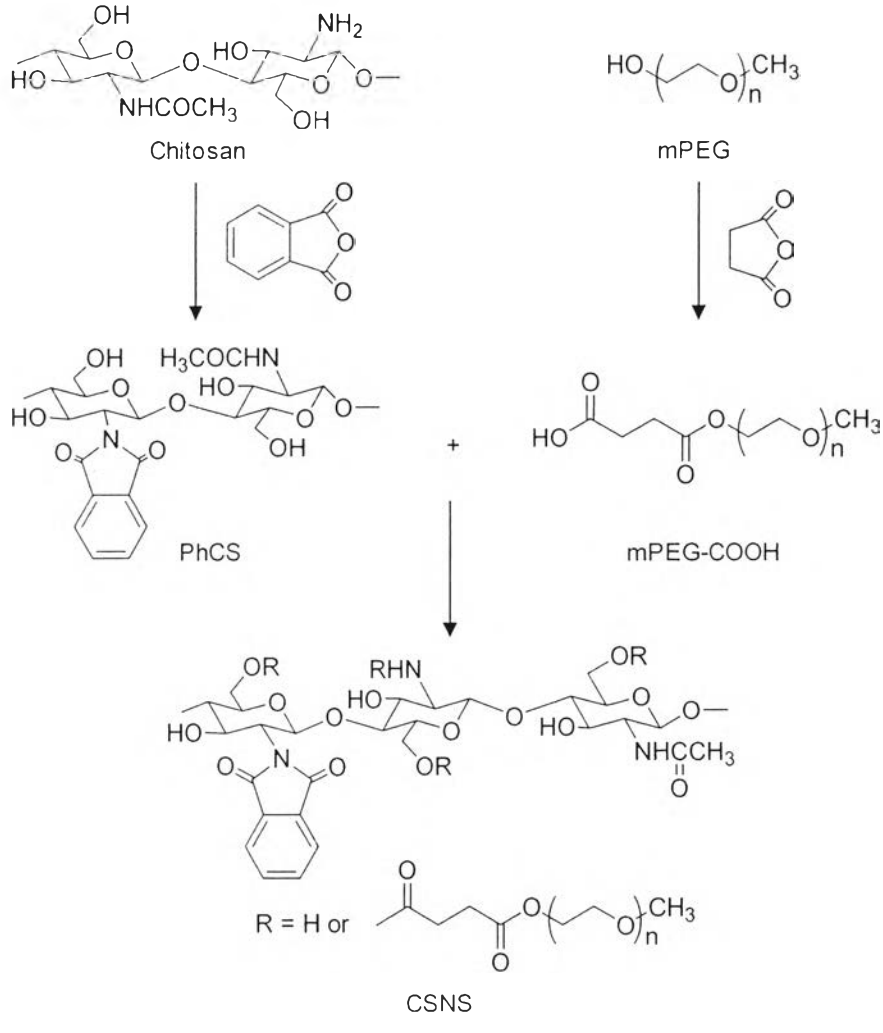

3.3.4 Preparation of CSNS-MAG and CSNS-O-MAG

CSNS (0.05 g) and MAG (0.05 g) were mixed in two types of aqueous solutions (10 mL): buffers, and de-ionized water. The buffers used were citrate buffer (pH 2.2), phosphate buffer (pH 3 to pH 8), and borate buffer (pH 9, and pH 10). In the case of de-ionized water, the pH was adjusted by adding HCl and

NaOH (0.1 mol L^{-1}). For all cases, CSNS-MAG in solutions were sonicated for 15 min before used.

For CSNS-OMAG, CSNS (0.05 g) was dissolved in DMF (5 mL), followed by adding O-MAG (0.004 g) to the solution with stirring at room temperature. The CSNS and O-MAG ratio was 1:0.05 (the MAG content was 60% of the weight of O-MAG). The mixture was dialyzed against DI water allowing the CSNS to reform a spherical structure.

3.3.5 Characterizations

A solution of CSNS-MAG hybrids were dispersed, resulting in concentration of 5×10^{-5} g mL^{-1}. Particles sizes and zeta potentials were measured by dynamic light scattering (DLS) using a Malvern Zetasizer Nano ZS at 25 °C. The morphologies were observed using a H-7650 TEM (Hitachi High-Technology Corporation, Japan) at an operating voltage of 100 kV. The stabilities of the hybrid colloidal solutions were evaluated by a Shimadzu UV-1800 spectrophotometer at 400 nm. The composition of CSNS-MAG was determined by a Perkin Elmer Pyris Diamond thermo gravimetric/ differential thermal analyzer (TG/DTA) under a heating range from 30 °C to 800 °C with a heating rate of 10 °C/min under a N_2 atmosphere. The N_2 flow rate was 100 mL min^{-1}. The data were averaged from three measurements.

3.4 Results and Discussion

3.4.1 Formation of CSNS-MAG and CSNS-O-MAG

The main question addressed in this study is whether or not the incorporation of MAG into CSNS relies on the hydrophilicity of MAG. Two types of nanoparticles, MAG and O-MAG, were used as CSNS guests. As the preparation of O-MAG was carried out by co-precipitating MAG under the presence of oleic acid, it was expected that O-MAG was hydrophobic and therefore it might be incorporated into CSNS's hydrophobic core.

Figure 3.1 (a) shows the chemical structure, TEM image, and schematic draw of CSNS which obtained from the colloidal solution in water. After simply mixing MAG with CSNS in an aqueous solution, CSNS-MAG was formed to give the particles to the side of CSNS indicating an existence of MAG on CSNS (Figure 3.1 (b)). Figure 3.1 (d) is a schematic of specific area (dotted block) demonstrating the formation of CSNS-MAG. The hydrophilic mPEG chains of CSNS might allow hydrophilic-hydrophilic interaction with MAG, resulting MAG surrounding the CSNS.

For O-MAG, both CSNS and O-MAG were dispersed in DMF followed by dialysis in water. This procedure was found to be effective in achieving incorporation of the hydrophobic compound, lidocaine, as reported previously [39]. Figure 3.1 (c) shows the dark particles surrounded by CSNS. This suggests the O-MAG in the inner area of CSNS. Figure 3.1 (e) illustrates the possible incorporation of MAG in CSNS at the hydrophobic core of phthalimido groups. The changes of MAG to O-MAG suggest how core-corona CSNS allows the interaction for both types of MAG.

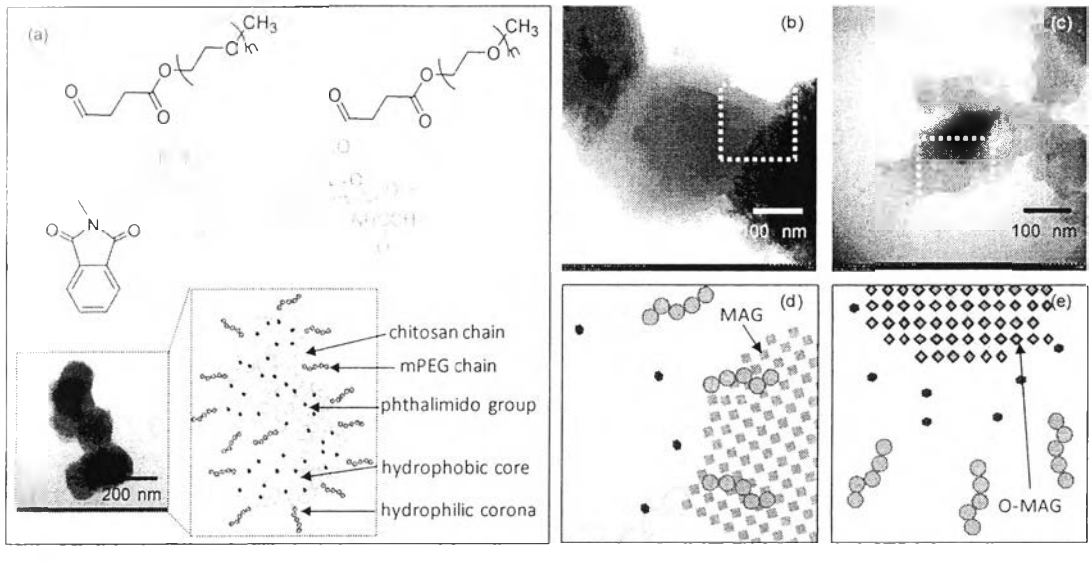

Figure 3.1 Chemical structure, TEM micrographs, and schematic draws of CSNS in water (a); TEM micrographs, and schematic draws of CSNS-MAG (b,d), and CSNS-O-MAG (c,e).

3.4.2 Solvent Polarity Effect on CSNS-MAG

As most applications of MAG are based in aqueous systems, an aqueous solution was used to prepare CSNS-MAG. Because the main factor governing the colloidal stability of CSNS is solvent polarity, the formation of CSNS-MAG under different solvents was investigated.

Figure 3.2 shows the relationship between the solvent polarity and the particle size diameter of CSNS-MAG (measured by DLS). It should be noted that the size evaluated by DLS is largely dependent on the behavior of the particles in solution. The solvents were categorized into polar protic solvents (water, and ethanol), polar aprotic solvents (DMF, and THF), and non-polar solvents (toluene). Colloidal formation was only observed in the polar protic solvents, water and ethanol, due to the relatively small size of the particles (~800 and ~1500 nm) compared to those in the aprotic solvents, DMF and THF, and in the non-polar solvent toluene, with particles being greater than 1500 nm in diameter. In other words, CSNS-MAG was well dispersed in the protic solvents and started to aggregate in the aprotic and non-polar solvents. This phenomenon is similar to that of CSNS, implying that the size of CSNS-MAG can be controlled by altering the solvent polarity.

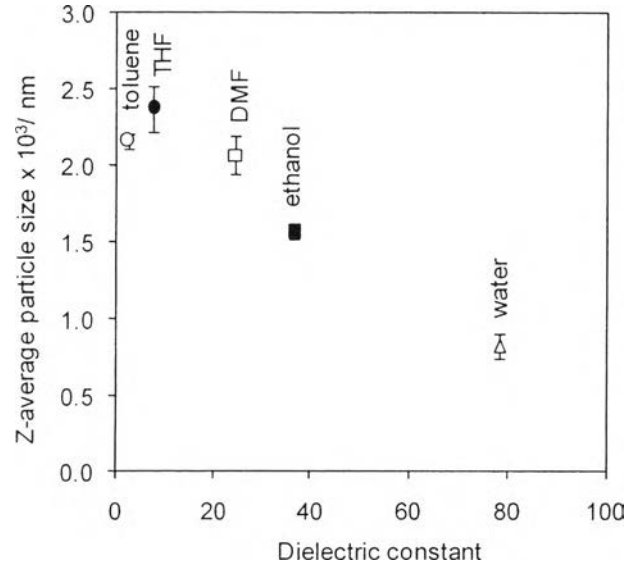

Figure 3.2 Z-average particle size of CSNS-MAG in toluene (○), THF (●), DMF (□), ethanol (■), and water (△).

It is important to note that when measuring CSNS-MAG size by DLS, it is difficult to trace when the nanoparticles start to aggregate, since a sudden precipitation might lead to a clear solution, resulting in the artifact reading of small particle sizes. For example, as shown in Figures 3.3 (a) – (c), in the case of CSNS-MAG in toluene, the supernatant is much clearer than that of water. In order to avoid the above-mentioned misinterpretation, the colloidal solution was dried and visualized by TEM (Figures 3.3 (d) – (f)). It should be noted that the use of TEM also helps us to observe how CSNS and MAG stabilize each other.

One question is why the sizes of CSNS are different in various solvents. The variation of size is related directly to the CSNS having a hydrophilic corona and a hydrophobic core, resulting in the responsiveness of the particles to the solvents. Therefore, in a hydrophobic solvent such as toluene, the PEG chain slightly pack, resulting in a significantly smaller size [29]. According to this, the dispersion of MAG for each solvent is largely dependent on the behavior of CSNS in each solvent. Figures 3.3 (g) – (i) are schematics that help to demonstrate this behavior.

In TEM images, the MAG can be identified as significant dark spots, compared to the gray spots of CSNS. When CSNS was dispersed in water, a stable colloidal solution (Figure 3.3 (a)) was obtained (see more information in the discussion of Figure 3.5). TEM micrograph confirms the presence of MAG as seen in Figure 3.3 (d). In the case of DMF (polar-aprotic solvent), the solution looks to have partial precipitation (Figure 3.3 (b)), whereas the TEM micrograph shows some MAG attached on the CSNS and some individually scattered (Figure 3.3 (e)). This suggests that the precipitation in Figure 3.3 (b) might be related to individual MAG. A similar but more significant phenomenon was seen with toluene. Here, the TEM micrograph confirms the individual existence of CSNS and MAG whereas the solution shows complete precipitation (Figure 3.3 (c)). The TEM micrographs confirm that the appearance of the solution state might be because of individual MAG which is not attached on the CSNS (Figure 3.3 (f)). Figures 3.3 (g)-(i) are schematics that illustrate the structures of CSNS-MAG in each solvent based on the information obtained from the TEM micrographs. The interaction of MAG on CSNS is largely dependent on the solvent. At that time, the protic solvent (water) seems to allow the interaction between the chitosan hydrophilic corona (mPEG moieties) and

the MAG. It should be noted that in the case of toluene, CSNS might have the phthalimido group on the surface, a condition that does not favor the interaction of MAG on the CSNS surface. This enables us to understand that CSNS-MAG stabilization is preferable in an aqueous system and allows us to control the size of CSNS-MAG, so that disintegration and precipitation can be prevented.

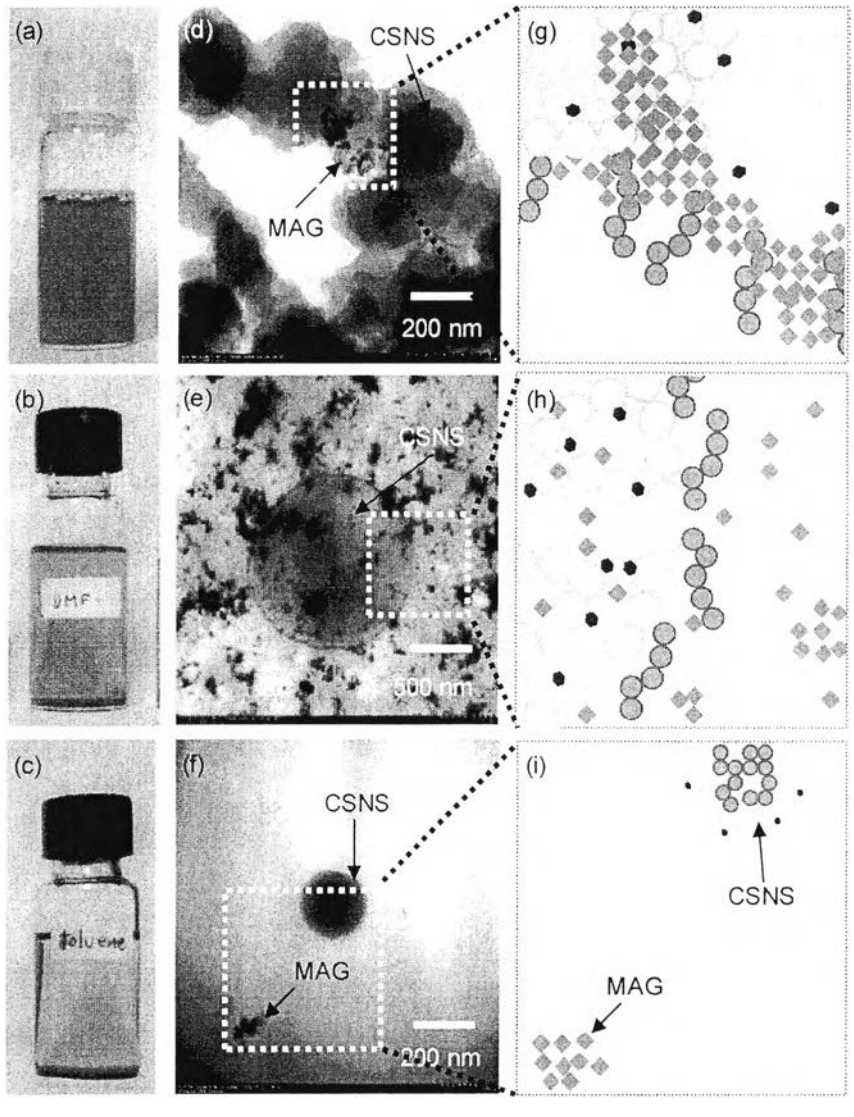

Figure 3.3 Photographs (left), TEM micrographs (middle), and schematic draws (right) of CSNS-MAG in water (a, d, g), DMF (b, e, h), and toluene (c, f, i).

In order to confirm that there is interaction between CSNS and MAG, the observation of CSNS-MAG in water containing various isopropanol contents was carried out. Figure 3.4 shows the particle size of colloidal particles as a function of the isopropanol content measured by DLS. As the percent of isopropanol is increased, the particle size increases from 800 nm - 900 nm to as high as ~2 μm (when the content of isopropanol in water was 60%). For over 40% isopropanol content in water, TEM images show the assembly of MAG and CSNS as clusters (Figure 3.4). This implies that the interaction between CSNS and MAG might be based on hydrogen bonding which becomes more significant when the polarity of the environment is decreased. It also indicates that the overall interaction between CSNS, MAG, and the solvent molecules controls particle aggregation.

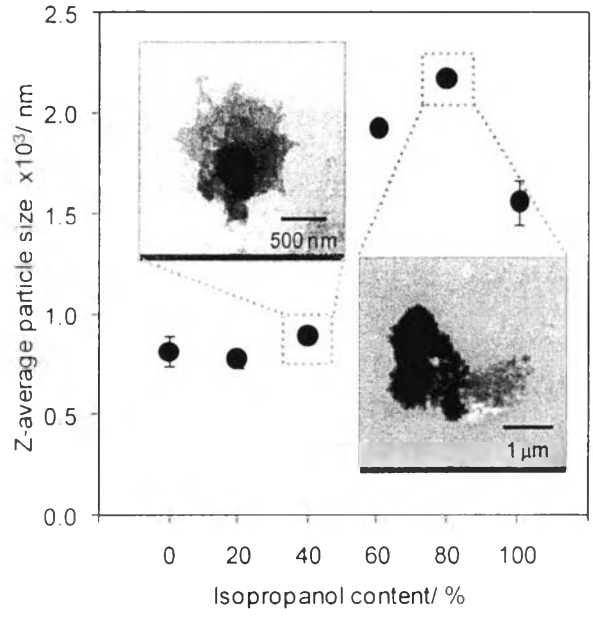

Figure 3.4 Z-average particle sizes of CSNS-MAG in water with various isopropanol contents.

3.4.3 pH Effects on CSNS-MAG

In most cases, the stabilization of MAG in aqueous solutions is difficult as MAG tends to aggregate and precipitate under these conditions. The equilibrium between attractive and repulsive forces is the key factor to achieve MAG

colloidal suspension. The attractive and repulsive forces in stabilizing MAG are: (i) van der Waals forces which induces strong short-distance isotropic attraction; (ii) electrostatic forces which is the force between two different or same charges particles; (iii) magnetic dipolar forces to induce anisotropic interactions; and (iv) steric repulsion forces among the particles [38].

Changing the pH using various buffers is a good way to control the attractive and repulsive forces mentioned above. It is noteworthy to mention that although the pH responsive phenomena such as colloidal stability and surface properties in the various buffer solutions were not dramatically obvious in the case of CSNS-MAG, the behavior of CSNS-MAG in various buffer solutions was still important to study. This is due to the fact that in most cases for biomolecular-involved studies, the experiments are usually conducted in buffer solutions to preserve fragile cells or to prevent protein denaturation.

In relation to the surface properties of CSNS-MAG nanoparticles in the buffer solutions, the main question was whether the salts in the buffer interrupt the interaction of the nanoparticles in the system. Figure 3.5 also shows the system of CSNS-MAG in de-ionized water. The pHs were adjusted by either HCl (aq) or NaOH (aq). Under these salt-free conditions, MAG show sizes (using DLS) in the range of 3000 nm to 4500 nm for all pHs, larger than CSNS or CSNS-MAG (Figure 3.5 (a)). This implies a strong aggregation of MAG in water. The surface charges of MAG are positive at a pH lower than 5, neutral at pH 6-7, and negative at pH 8-10 (Figure 3.5 (b)). This reflects how the surface of MAG could be easily changed by controlling the pH.

For CSNS at pH 2 - pH 4 and at pH 10, the sizes measured using DLS are ~2000 nm, whereas from pH 6 to pH 9, the sizes decreased to 1000 nm. The zeta potential indicates that in highly acidic pHs, CSNS is positively charged, becoming neutral at pH 5 and negatively charged at higher pHs.

Based on the observations of isolated MAG and CSNS, the sizes and charges of CSNS-MAG should reflect the interaction between CSNS and MAG in aqueous system. It should be noted that CSNS-MAG have smaller particle sizes than MAG (but close to CSNS), as measured by DLS, especially between pH 6 to pH 9. CSNS-MAG decreases its size down to ~1000 nm when the conditions were changed

from acidic to basic, indicating the pH responsiveness of CSNS-MAG. It should be noted however, that MAG tends to be instable in strong acidic or alkaline conditions. The performance in neutral pHs support the stability of MAG as well as its effective coverage on CSNS. Figure 3.5 (b) shows that CSNS-MAG has a negative charge which might be solely related to the MAG, even when combined with CSNS.

A TEM micrograph (Figure 3.5 (c)) clearly identifies that in acidic pHs, MAG tends to aggregate, even when attached on CSNS surfaces. However, in a neutral pH (Figure 3.5 (d)), it can be seen that MAG (dark dots) are dispersed on the CSNS. Figures 3.5 (e) and (f) are schematics that illustrate the structures of CSNS-MAG in various pH conditions based on the surface properties measured and the information gained from TEM micrographs. It has been shown that by varying the pH, the particle size of CSNS-MAG nanoparticles and the MAG responsiveness can be controlled. Moreover, the preferable small particle sizes and effective coverage of MAG on CSNS are found at neutral pHs, a more suitable pH for biological applications.

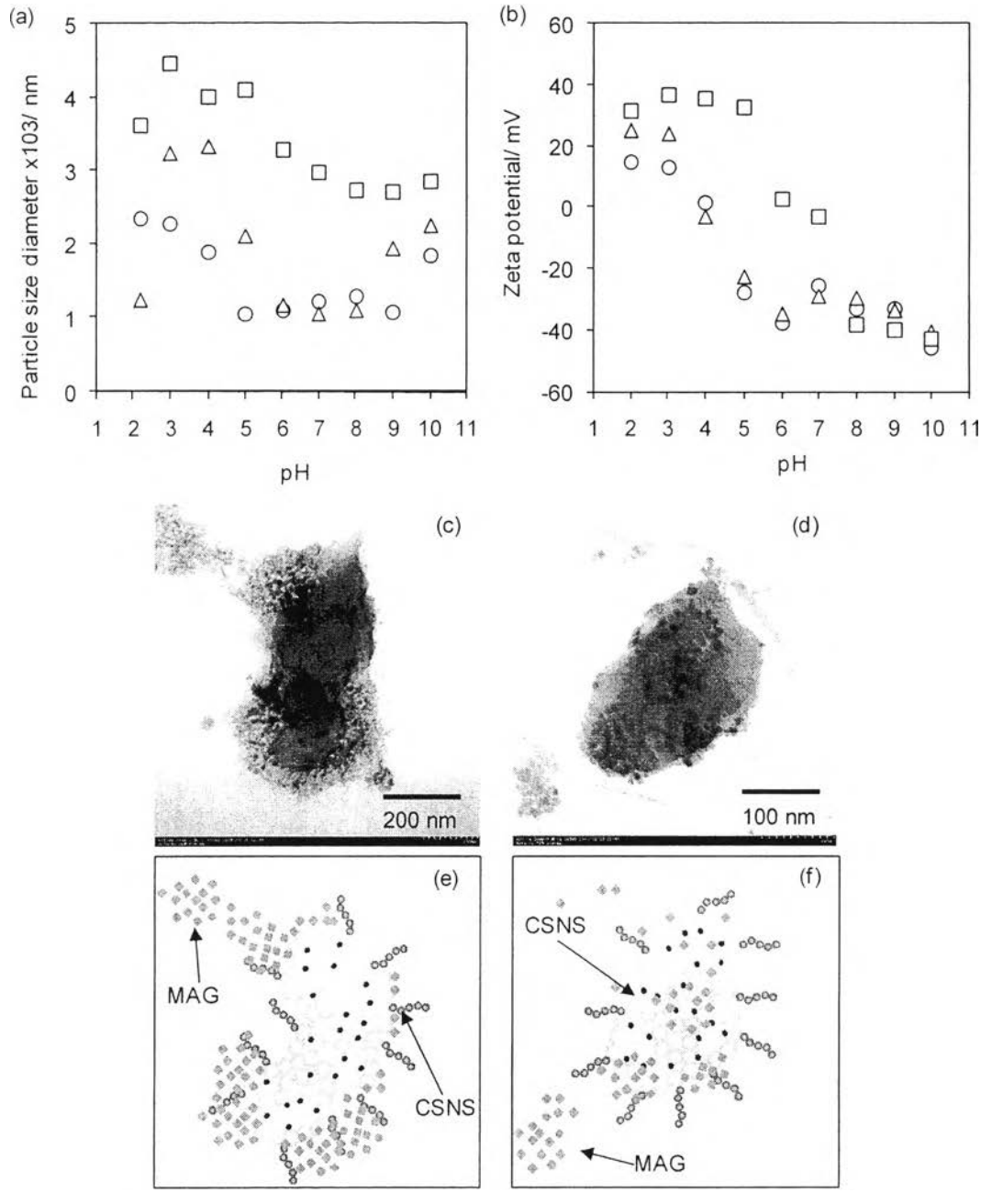

Figure 3.5 Particle size (a) and zeta potential (b) of CSNS (○), MAG (□), and CSNS-MAG (△) in (pH adjusted) water from pH 2.2 to pH 10; TEM images of CSNS-MAG in (pH adjusted) water pH 3 (c), and pH 6 (d); schematic draws of CSNS-MAG in acidic or basic pHs (e), and neutral pH (f).

3.4.4 Control of MAG Content on CSNS by pH Responsiveness

It is important to investigate the amount of MAG which can cover CSNS at different pHs. Here, to purify the CSNS-MAG, the free MAG was removed by an external strong magnet. As the free MAG easily attaches to the magnet, this purification step was successful.

The amount of MAG attached onto CSNS can be traced by TG/DTA by following the degradation of CSNS-MAG. The degradation of CSNS-MAG prepared in aqueous solution at various pHs were evaluated as follows. Decomposition of CSNS was found to occur between 200–600 °C. The content of CSNS (%wt) was calculated in the temperature range of 150 °C to 600 °C including 5%wt of ash content. A 5%wt of ash content was assumed based on the TG/DTA result of pure CSNS (see Supporting Information Figure S3). As MAG showed no degradation, the MAG content could be traced by the %wt remained after heating to 600 °C. The contents of CSNS and MAG in CSNS-MAG at various pHs are summarized in Table 3.1.

Table 3.1 Content of CSNS and MAG in CSNS-MAG

Conditions*	%CSNS	%MAG	CSNS/MAG (by %wt)
pH 2	66.3±5.5	33.7±5.5	2.1±0.5
pH 4	72.7±3.3	27.3±3.3	2.8±0.5
pH 6	61.6±3.3	38.4±4.6	1.7±0.3
pH 10	49.8±2.2	50.2±2.2	1.0±0.1

*pHs were adjusted by HCl (aq) or NaOH (aq).

Table 3.1 shows high MAG contents at a pH 6. This might be due to the opposite charge of MAG and CSNS at this pH, as identified from Figure 3.5. At pH 10, it was unexpected to see such a high content of MAG. Although the reason is not clear, TEM micrograph also confirmed the high content for this pH.

It is important to note that ideally, the applications of magnetic nanoparticles require colloidal stability and magnetic responsiveness. While most

commercial magnetic nanoparticulates are stable in aqueous solutions for only a few minutes, the CSNS-MAG maintains its colloidal stability for 2-3 hours (see 3.4.3 pH effects on CSNS-MAG). Based on the responsiveness of MAG, variation of the pH allows us to control the MAG content of CSNS-MAG.

3.5 Conclusions

CSNS, with its hydrophobic core and hydrophilic corona is a convenient material allowing the stabilization of hydrophilic MAG and hydrophobic O-MAG. By simply mixing CSNS with two types of MAG in aqueous solution, the CSNS-MAG and CSNS-O-MAG were easily formed. In the case of O-MAG, the phthalimido group played an important role to incorporate the O-MAG at the core. The m-PEG chains of CSNS interact with MAG, resulting in the stabilization of MAG on the surface. The fact that CSNS-MAG is responsive to the polarity and pH of the solvent leads to two advantages: (i) the particle size is adjustable; and (ii) the MAG content is controllable. The present work demonstrates a model case for when polymer chains are in core-corona structure, a structure affected by the solvent polarity and/or pH; the simple mixing with inorganic nanoparticles will allow us to tailor inorganic nanoparticulate polymers with desired specifications.

3.6 Acknowledgements

One of the authors (S. Chatrabhuti) would like to acknowledge the Center for Petroleum, Petrochemical and Advanced Materials, the Petroleum and Petrochemical College, Chulalongkorn University for the Ph.D. scholarship. This work was supported by the Research, Development and Engineering (RD&E) fund through the National Nanotechnology Center (NANOTEC), the National Science and Technology Development Agency (NSTDA), Thailand (Project No.NN-B-22-FN1-10-52-14) to the Petroleum and Petrochemical College. Gratitude is also extended to the National Research Council of Thailand (NRCT) and the Integrated Innovation Academic Center: IIAC Chulalongkorn University Centenary Academic Development Project. Chitosan was kindly supplied by Seafresh Chitosan (Lab)

Company Limited, Thailand. The authors gratefully thank the Hitachi High Technologies for TEM measurements. The authors thank Dr. Surachai Ngamratanapaiboon, Department of Biochemistry, Faculty of Pharmacy, Mahidol University for his help in DNA extraction study. The authors would like to extend their special thank to Professor Robert G. Gilbert and Mitchell Sullivan, Queensland Alliance for Agriculture & Food Innovations University of Queensland, Australia for the valuable comments and English corrections.

3.7 References

1. Lee H-Y, Li Z, Chen K, Hsu AR, Xu C, Xie J, Sun S, and Chen X. Journal of Nuclear Medicine 2008.
2. Lübbe AS, Alexiou C, and Bergemann C. Journal of Surgical Research 2001;95(2):200-206.
3. Liu J, Wang B, Budi Hartono S, Liu T, Kantharidis P, Middelberg APJ, Lu GQ, He L, and Qiao SZ. Biomaterials 2012;33(3):970-978.
4. Li Z, Yi PW, Sun Q, Lei H, Li Zhao H, Zhu ZH, Smith SC, Lan MB, and Lu GQ. Advanced Functional Materials 2012;22(11):2387-2393.
5. Denkbaş EB, Kiliçay E, Birlikseven C, and Öztürk E. Reactive and Functional Polymers 2002;50(3):225-232.
6. Hritcu D, Popa MI, Popa N, Badescu V, and Balan V. Turkish Journal of Chemistry 2009;33(6):785-796.
7. Xie J, Chen K, Lee H-Y, Xu C, Hsu AR, Peng S, Chen X, and Sun S. Journal of the American Chemical Society 2008;130(24):7542-7543.
8. Cao H, He J, Deng L, and Gao X. Applied Surface Science 2009;255(18):7974-7980.
9. Mahmoudi M, Simchi A, Imani M, Milani AS, and Stroeve P. The Journal of Physical Chemistry B 2008;112(46):14470-14481.
10. Ji Zhang, Shengtang Zhang, Guangpeng Wu, Wenqiang Wang, Sufang Gao, and Yunpu Wang. Journal of Bioactive and Compatible Polymers 2007;22(4):429-441.

11. Namdeo M and Bajpai SK. Colloids and Surfaces A: Physicochemical and Engineering Aspects 2008;320(1–3):161-168.
12. Čampelj S, Makovec D, and Drofenik M. Journal of Magnetism and Magnetic Materials 2009;321(10):1346-1350.
13. Wang J, Meng G, Tao K, Feng M, Zhao X, Li Z, Xu H, Xia D, and Lu JR. PLoS ONE 2012;7(8):e43478.
14. De Palma R, Peeters S, Van Bael MJ, Van den Rul H, Bonroy K, Laureyn W, Mullens J, Borghs G, and Maes G. Chemistry of Materials 2007;19(7):1821-1831.
15. Yuan Q, Venkatasubramanian R, Hein S, and Misra RDK. Acta Biomaterialia 2008;4(4):1024-1037.
16. Liu X, Guan Y, Ma Z, and Liu H. Langmuir 2004;20(23):10278-10282.
17. Ge Y, Zhang S, He S, Zhang Y, and Gu N. Journal of Nanoscience and Nanotechnology 2009;9(2):1287-1290.
18. Liu X, Hu Q, Fang Z, Zhang X, and Zhang B. Langmuir 2008;25(1):3-8.
19. Finotelli PV, Da Silva D, Sola-Penna M, Rossi AM, Farina M, Andrade LR, Takeuchi AY, and Rocha-Leão MH. Colloids and Surfaces B: Biointerfaces 2010;81(1):206-211.
20. Šafařı, amp, x, ková M, Roy I, Gupta MN, and k I. Journal of Biotechnology 2003;105(3):255-260.
21. El-Dakdouki MH, El-Boubbou K, Zhu DC, and Huang X. RSC Advances 2011;1(8):1449-1452.
22. Liu L, Yang J-P, Ju X-J, Xie R, Liu Y-M, Wang W, Zhang J-J, Niu CH, and Chu L-Y. Soft Matter 2011;7(10):4821-4827.
23. Amoozgar Z, Park J, Lin Q, and Yeo Y. Molecular Pharmaceutics 2012;9(5):1262-1270.
24. Krishna Rao KSV, Vijaya Kumar Naidu B, Subha MCS, Sairam M, and Aminabhavi TM. Carbohydrate Polymers 2006;66(3):333-344.
25. Popat A, Liu J, Lu GQ, and Qiao SZ. Journal of Materials Chemistry 2012;22(22):11173-11178.
26. Sashiwa H, Kawasaki N, Nakayama A, Muraki E, Yamamoto N, and Aiba S-i. Biomacromolecules 2002;3(5):1126-1128.

27. Chirachanchai S and Fangkangwanwong J. Chitosan Water-Soluble System: An Approach to Prepare Superabsorbent Gel. Polymers for Biomedical Applications, vol. 977: American Chemical Society, 2008. pp. 27-36.
28. Cho J, Grant J, Piquette-Miller M, and Allen C. Biomacromolecules 2006;7(10):2845-2855.
29. Fangkangwanwong J, Akashi M, Kida T, and Chirachanchai S. Macromolecular Rapid Communications 2006;27(13):1039-1046.
30. Phongying S, Aiba S-i, and Chirachanchai S. Polymer 2007;48(1):393-400.
31. Yoksan R, Akashi M, Hiwatari K-i, and Chirachanchai S. Biopolymers 2003;69(3):386-390.
32. Yoksan R, Matsusaki M, Akashi M, and Chirachanchai S. Colloid & Polymer Science 2004;282(4):337-342.
33. Nishimura S, Kohgo O, Kurita K, and Kuzuhara H. Macromolecules 1991;24(17):4745-4748.
34. Chirachanchai S, Lertworasirikul A, and Tachaboonyakiat W. Carbohydrate Polymers 2001;46(1):19-27.
35. Chen L, Tian Z, and Du Y. Biomaterials 2004;25(17):3725-3732.
36. Srakaew V, Ruangsri P, Suthin K, Thunyakitpisal P, and Tachaboonyakiat W. Journal of Biomaterials Applications 2012;27(4):403-412.
37. Tachaboonyakiat W, Netswasdi N, Srakaew V, and Opaprakasit M. Polymer Journal 2010;42(2):148-156.
38. Zhang C, Ping Q, Zhang H, and Shen J. European Polymer Journal 2003;39(8):1629-1634.
39. Choochottiros C, Yoksan R, and Chirachanchai S. Polymer 2009;50(8):1877-1886.
40. Opanasopit P, Ngawhirunpat T, Rojanarata T, Choochottiros C, and Chirachanchai S. Colloids and Surfaces B: Biointerfaces 2007;60(1):117-124.
41. Belessi V, Zboril R, Tucek J, Mashlan M, Tzitzios V, and Petridis D. Chemistry of Materials 2008;20(10):3298-3305.
42. Bhattarai SR, Kc RB, Kim SY, Sharma M, Khil MS, Hwang PH, Chung GH, and Kim HY. Journal of nanobiotechnology 2008;6:1.

43. Zhi J, Wang Y, Lu Y, Ma J, and Luo G. Reactive and Functional Polymers 2006;66(12):1552-1558.

44. Laurent S, Forge D, Port M, Roch A, Robic C, Vander Elst L, and Muller RN. Chemical Reviews 2008;108(6):2064-2110.